

---

# One Brain, Omni Modalities: Towards Unified Non-Invasive Brain Decoding with Large Language Models

---

Changli Tang<sup>3</sup> Shurui Li<sup>1,2</sup> Junliang Wang<sup>1</sup> Qinfan Xiao<sup>1,3</sup> Zhonghao Zhai<sup>3</sup> Lei Bai<sup>1</sup> Yu Qiao<sup>1</sup>  
Bowen Zhou<sup>1,3</sup> Wen Wu<sup>1</sup> Yuanning Li<sup>1,2</sup> Chao Zhang<sup>1,3</sup>

## Abstract

Deciphering brain function through non-invasive recordings requires synthesizing complementary high-frequency electromagnetic (EEG/MEG) and low-frequency metabolic (fMRI) signals. However, despite their shared neural origins, extreme discrepancies have traditionally confined these modalities to isolated analysis pipelines, hindering a holistic interpretation of brain activity. To bridge this fragmentation, we introduce **NOBEL**, a **neuro-omni-modal brain-encoding large language model (LLM)** that unifies these heterogeneous signals within the LLM’s semantic embedding space. Our architecture integrates a unified encoder for EEG and MEG with a novel dual-path strategy for fMRI, aligning non-invasive brain signals and external sensory stimuli into a shared token space, then leverages an LLM as a universal backbone. Extensive evaluations demonstrate that NOBEL serves as a robust generalist across standard single-modal tasks. We also show that the synergistic fusion of electromagnetic and metabolic signals yields higher decoding accuracy than unimodal baselines, validating the complementary nature of multiple neural modalities. Furthermore, NOBEL exhibits strong capabilities in stimulus-aware decoding, effectively interpreting visual semantics from multi-subject fMRI data on the NSD and HAD datasets while uniquely leveraging direct stimulus inputs to verify causal links between sensory signals and neural responses. NOBEL thus takes a step towards unifying non-invasive brain decoding, demonstrating the promising potential of omni-modal brain understanding.

## 1. Introduction

The human brain operates as an intricate biological processor, orchestrating complex neural activities that encode our perceptions, thoughts, and physiological states. To non-invasively decipher these mechanisms, researchers primarily rely on two distinct categories of signals: high-frequency electromagnetic fluctuations arising from neuronal firing, captured via electroencephalography (EEG) and magnetoencephalography (MEG), and low-frequency metabolic changes reflecting hemodynamic responses, captured via functional magnetic resonance imaging (fMRI). Driven by the success of representation learning, recent years have witnessed a surge in foundation models tailored for these individual modalities. Significant progress has been made in building specialized models for EEG (Xiao et al., 2025; Peh et al., 2022; Song et al., 2021; Jing et al., 2023; Yang et al., 2023; Jiang et al., 2024; Wang et al., 2025b; Ouahidi et al., 2025; Yi et al., 2023), MEG (Xiao et al., 2025; Hirano et al., 2024), and fMRI (Wang et al., 2025a; Scotti et al., 2024; Kawahara et al., 2017; Li et al., 2021; Kan et al., 2022b;a; Wei et al., 2025; Dong et al., 2025; Kim et al., 2023; Ozcelik & VanRullen, 2023; Scotti et al., 2023; Chen et al., 2025; Tang et al., 2023; Horikawa, 2025; Fu et al., 2025; Takagi & Nishimoto, 2023), each demonstrating strong capabilities in decoding specific aspects of brain function.

Despite these advances, the field remains fragmented. While electromagnetic and metabolic signals are merely different manifestations of the same underlying neural processes, they are traditionally treated as isolated domains due to their extreme heterogeneity. EEG and MEG offer millisecond-level temporal resolution but poor spatial localization, whereas fMRI provides rich spatial details but suffers from significant temporal lag. Theoretically, a unified analysis of these complementary modalities could unlock a holistic view of brain dynamics, yet current frameworks lack the capability to bridge this “frequency gap” effectively. Furthermore, neural activity does not occur in a vacuum; it is deeply grounded in the external sensory environment. However, most of recent brain foundation models aim to learn task-agnostic neural representations and therefore do not explicitly incorporate task-specific or stimulus-level contextual information.

---

<sup>1</sup>Shanghai AI Laboratory <sup>2</sup>ShanghaiTech University  
<sup>3</sup>Tsinghua University. Correspondence to: Chao Zhang  
<cz277@tsinghua.edu.cn>.

As a result, the rich structure of the evoking stimuli is often underutilized during representation learning. Integrating these external stimuli as contextual input is crucial, as it provides the ground truth necessary to align complex brain signals with high-level semantic concepts, thereby raising the ceiling of decoding performance.

To address these challenges, we introduce NOBEL, a neuro-omni-modal brain-encoding LLM designed to bridge the chasm between high-frequency electromagnetic activities, low-frequency metabolic states, and external sensory stimuli. We conceptualize brain signal decoding as a multi-modal alignment problem, leveraging the strong LLMs to integrate heterogeneous data sources. Specifically, NOBEL employs a modular encoding strategy to project diverse signals into a shared semantic space compatible with the LLM. For high-frequency data, BrainOmni (Xiao et al., 2025) is used to extract temporal features from EEG and MEG. For fMRI signals, we propose a novel dual-path encoding mechanism, employing NeuroSTORM (Wang et al., 2025a) to capture global, static subject-dependent meta-information and the MindEye2 structure (Scotti et al., 2024) to extract dynamic, stimulus-evoked perceptual features. By simultaneously ingesting these brain signals alongside the corresponding visual or auditory stimuli, NOBEL translates multi-modal inputs into unified tokens, allowing users to control decoding tasks and generate insights via natural language prompts.

Our contributions are summarized as follows:

- **First Omni-Modal Brain Foundation Model:** We present NOBEL, a unified framework that supports EEG, MEG, and fMRI processing. By orchestrating these heterogeneous signals within a single LLM, NOBEL achieves competitive performance across a wide range of benchmarks compared to modality-specific specialists.
- **Novel Dual-Path fMRI Encoding:** We propose a hybrid encoding architecture specifically optimized for metabolic signals to disentangle the extraction of static physiological meta-information from dynamic, stimuli-responsive features, which effectively capturing the rich spatiotemporal information embedded in low-frequency fMRI data.
- **Stimuli-Aware Task Generalization:** We demonstrate that NOBEL not only effectively performs stimuli decoding tasks but is also able to leverage external audio-visual stimuli as contextual anchors to tackle tasks beyond the reach of previous models, such as verifying whether a subject is perceiving a specific target image or video.

The rest of the paper is structured in the following manner. Section 2 reviews existing research and foundation models for EEG/MEG and fMRI signals. Section 3 details the methodology of NOBEL, describing the unified model architecture and the multi-stage training pipeline. Section 4

provides the experimental setup, including data specifications and implementation details. Section 5 presents comprehensive experimental results. We conclude in Section 6.

## 2. Related Work

### 2.1. Foundation Models for EEG and MEG Signals

The analysis of non-invasive high-frequency electromagnetic brain signals, specifically EEG and MEG, has historically been challenged by low signal-to-noise ratios (SNRs) and the complex spatial-temporal dynamics of neuronal firing. Early deep learning approaches predominantly focused on designing specialized architectures to tackle specific clinical tasks. For instance, CNN-Transformer (Peh et al., 2022) integrated CNNs for local feature extraction with Transformers for global context to automate artifact detection, while ST-Transformer (Song et al., 2021) utilized a similar hybrid structure to decode spatial-temporal features from EEG. In clinical settings, SPARCNet (Jing et al., 2023) demonstrated that dense convolutional networks could achieve expert-level performance in classifying seizures and rhythmic periodic patterns. Similarly, in the MEG domain, FAMED (Hirano et al., 2024) employed deep learning for the automatic detection and dipole estimation of epileptic discharges, proving the efficacy of deep networks in magnetic signal analysis.

Despite the success of these supervised methods, their reliance on extensive annotated data limited their scalability. This led to a shift towards self-supervised learning (SSL), where models learn robust representations from unlabeled data. MMM (Yi et al., 2023) maps any EEG channel distribution into a unified topology and conducts multi-stage pre-training. ContraWR (Yang et al., 2023) applies contrastive learning to EEG, enabling automated sleep staging with reduced reliance on labeled experts. LaBraM (Jiang et al., 2024) further scaled pre-training through vector-quantized neural spectrum prediction. More recently, CBraMod (Wang et al., 2025b) introduced a criss-cross attention mechanism to better capture the orthogonal relationships between spatial and temporal dimensions in EEG data. REVE (Ouahidi et al., 2025) utilized a 4D positional encoding scheme to process signals of any length and electrode arrangement.

Notably, neuronal activity underpins human brain function by generating electrical currents in the cortex, which in turn produce secondary electrical and magnetic fields measurable by EEG and MEG. Although these signals stem from the same underlying neural sources, previous foundation models have largely ignored this biophysical unity and treated electric and magnetic modalities as separate domains. The recently proposed BrainOmni (Xiao et al., 2025) bridges this gap by mapping diverse sensor configurations into a shared latent space and establishes a unified EMEG encoder.

## 2.2. Foundation Models for fMRI Signals

While EEG and MEG capture rapid neural dynamics, fMRI provides spatially resolved metabolic insights. The development of deep learning models for fMRI has largely been dictated by data representation strategies. Traditionally, to mitigate the curse of dimensionality, fMRI data is reduced to region-of-interest (ROI)-level time-series extracted from pre-defined brain atlases. From these time-series, various low-dimensional matrix representations like functional connectivity or functional gradients can be derived, which summarize inter-regional relationships. Early supervised models treated these matrix representations as grid-like structures or graphs; for instance, BrainNetCNN (Kawahara et al., 2017) pioneered the use of specialized convolutional filters to capture topological features, while subsequent works like BrainGNN (Li et al., 2021) and FBNETGEN (Kan et al., 2022a) adopted graph neural networks to improve interpretability and task-aware network generation. With the advent of Transformers, architectures such as the Brain Network Transformer (Kan et al., 2022b) were proposed to learn pair-wise connection strengths among ROI by utilizing connection profiles as node features and incorporating an orthonormal clustering readout. Recent efforts have attempted to scale this paradigm to foundation model settings, with Brain Harmony (Dong et al., 2025) aligning multi-site data via unified ROI embeddings and fMRI-LM (Wei et al., 2025) exploring the intersection of ROI sequences and language models. However, these ROI-based methods suffer from a fundamental bottleneck: the reliance on fixed atlases introduces rigid inductive biases and inconsistent preprocessing pipelines, limiting their ability to generalize across datasets processed with different parcellation schemes.

In contrast, directly modeling raw 4D voxel data offers a promising alternative that avoids manual parcellation and preserves fine-grained neural information. This volume-based paradigm treats fMRI as dense spatiotemporal videos rather than simplified graphs. SWiFT (Kim et al., 2023) successfully applied Swin Transformers to 4D fMRI clips, showing the feasibility of learning hierarchical spatiotemporal representations without manual feature engineering. Pushing this direction further, NeuroSTORM (Wang et al., 2025a) extracts robust, fine-grained voxel features that generalize well to downstream tasks such as phenotype prediction and disease diagnosis, by pre-training on massive multi-subject datasets using masked autoencoding.

Distinct from methods that primarily focus on analyzing physiological states, a parallel stream of research aims to explicitly decode perceptual content, such as decoding visual or auditory stimuli from brain activity. For decoding continuous stimuli (e.g. long natural speech or videos), models (Tang et al., 2023; Fu et al., 2025) typically operate directly on the fMRI time series to translate fMRI signals into per-

ceived continuous stimuli. In contrast, for event-related stimuli, event-related neural representations are commonly used, such as general linear model (GLM)-derived beta weights (Takagi & Nishimoto, 2023) or trial-averaged activations (Chen et al., 2025; Horikawa, 2025), focusing on the semantic alignment between brain activity and external stimuli. Generative approaches like BrainDiffuser (Ozcelik & VanRullen, 2023) and MindEye (Scotti et al., 2023) are also based on beta weights and have achieved superior results in reconstructing perceived images by aligning fMRI embeddings with the latent spaces of diffusion models such as CLIP (Radford et al., 2021). Similarly, NeuroBind (Yang et al., 2024) leverages CLIP embeddings as a universal anchor to unify diverse neural modalities into a shared semantic space. The recently proposed MindEye2 (Scotti et al., 2024) further enhances the neural-visual alignment, enabling high-fidelity reconstruction with less training data.

## 3. Methodology

### 3.1. Model Architecture

NOBEL is a unified foundation model designed to decode omni-modal non-invasive brain signals, ranging from low-frequency fMRI activities to high-frequency EEG and MEG signals, within a shared semantic space. As illustrated in Fig. 1, the framework operates as a general-purpose interpreter, which accepts a flexible combination of fMRI, EEG, MEG, and external stimuli, controlled via user-provided textual prompts to generate natural language responses. To maintain signal granularity and task flexibility, fMRI signals are processed as raw 4D voxels and GLM beta weights.

To bridge the substantial domain gap between biological signals and the LLM’s textual embedding space, we design specialized encoding streams that converge via a unified alignment mechanism. For metabolic signals, we implement a dual-path strategy to explicitly disentangle physiological state information from task-related semantic information. The first path is *task-agnostic*, designed to capture universal physiological features embedded in raw voxels. We employ a universal encoder  $\mathcal{E}_{\text{vox}}$  based on NeuroSTORM (Wang et al., 2025a) to process the raw 4D input  $\mathbf{X}_{\text{vox}}$ . The second path is *task-specific*, aiming to extract high-level semantic content from GLM beta weights. Recognizing that semantic representations vary significantly across different modalities (e.g., viewing an image and watching a video), we instantiate a set of task-specific encoders  $\{\mathcal{E}_{\text{beta}}^{(k)}\}_{k=1}^K$ , where each encoder corresponds to a specific stimulus domain  $k$ . To map these heterogeneous features into the LLM’s input space, each encoding branch is followed by a modality aligner  $\text{Aligner}(\cdot)$ , implemented as a 3-layer multilayer perceptron (MLP) with GELU activation (Hendrycks & Gimpel, 2016). Consequently, the unified metabolic tokens  $\mathbf{H}_{\text{vox}}$  and the

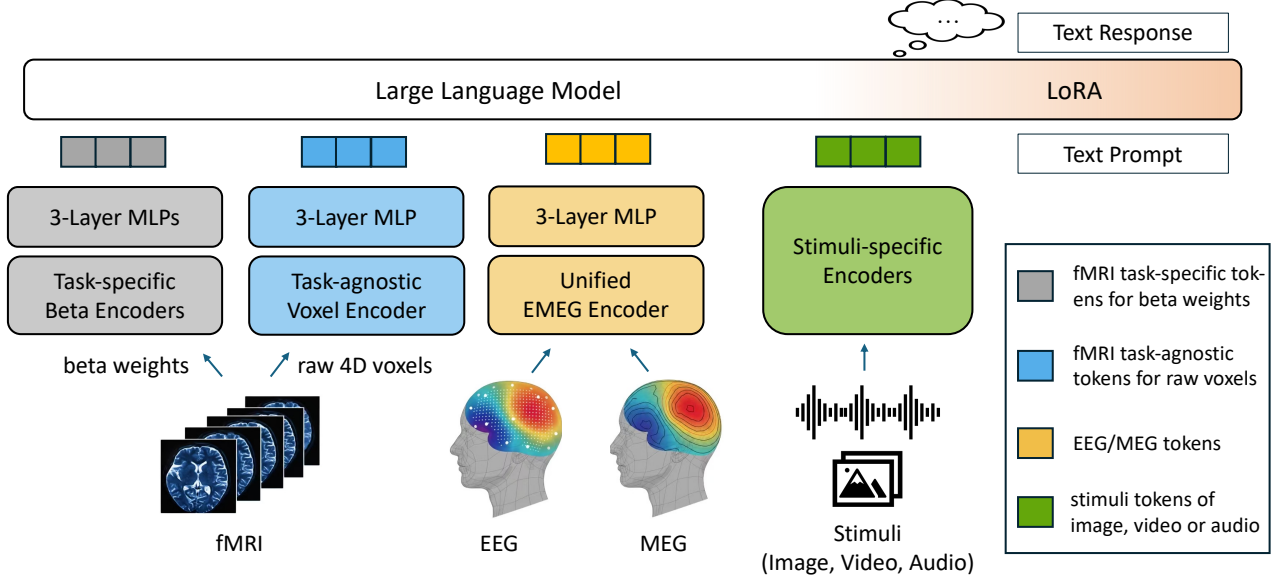


Figure 1. Overview of the NOBEL architecture. The model integrates heterogeneous brain signals and external stimuli into an LLM, features dual-path fMRI encoders for disentangling metabolic features (raw voxels vs. beta weights) and a unified EEG/MEG encoder for electromagnetic dynamics. All brain modalities are projected into the LLM’s input space via modality-specific 3-Layer MLP aligners. The system supports flexible input combinations and is optimized via LoRA for instruction-following tasks.

task-specific semantic tokens  $\mathbf{H}_{\text{beta}}^{(k)}$  are formally derived as:

$$\mathbf{H}_{\text{vox}} = \text{Aligner}_{\text{vox}}(\mathcal{E}_{\text{vox}}(\mathbf{X}_{\text{vox}})), \quad (1)$$

$$\mathbf{H}_{\text{beta}}^{(k)} = \text{Aligner}_{\text{beta}}^{(k)}(\mathcal{E}_{\text{beta}}^{(k)}(\mathbf{X}_{\text{beta}}^{(k)})). \quad (2)$$

where  $\mathbf{X}_{\text{beta}}^{(k)}$  denotes the beta weights associated with the  $k$ -th task. This design allows NOBEL to simultaneously leverage global physiological context and precise, stimulus-aligned semantic details.

Complementing the metabolic perspective, we model high-frequency electromagnetic signals using a unified EEG/MEG encoder. Although EEG and MEG measure different physical quantities (electrical potentials and magnetic flux, respectively), both arise from the same underlying neuronal current sources. Exploiting this shared biophysical origin, we adopt the BrainOmni backbone  $\mathcal{E}_{\text{em}}$  to extract unified temporal-spectral representations from the input sequence  $\mathbf{X}_{\text{em}}$ . The resulting electromagnetic tokens  $\mathbf{H}_{\text{em}}$  are then mapped into the semantic space of the LLM through a modality-specific three-layer MLP aligner as:

$$\mathbf{H}_{\text{em}} = \text{Aligner}_{\text{em}}(\mathcal{E}_{\text{em}}(\mathbf{X}_{\text{em}})). \quad (3)$$

Furthermore, to ground these abstract neural representations in their perceptual context, the model incorporates external stimuli via a stimuli-aware encoding stream. Similar to the task-specific fMRI path, distinct encoders  $\mathcal{E}_{\text{stim}}^{(m)}$  are employed for different stimulus modalities  $m$  (e.g., visual or audio) to process the raw media inputs  $\mathbf{X}_{\text{stim}}^{(m)}$ . The modality-specific stimulus tokens  $\mathbf{H}_{\text{stim}}^{(m)}$  are obtained as:

$$\mathbf{H}_{\text{stim}}^{(m)} = \mathcal{E}_{\text{stim}}^{(m)}(\mathbf{X}_{\text{stim}}^{(m)}). \quad (4)$$

The integration framework is inherently flexible, allowing NOBEL to process arbitrary combinations of available inputs. We dynamically construct the LLM-input sequence  $\mathbf{S}$  by concatenating the user prompt  $\mathbf{T}_{\text{prompt}}$  with the aligned tokens of all present modalities. Let  $\mathcal{M}$  and  $\mathcal{K}$  denote the sets of available stimulus modalities and task-specific beta inputs, and let  $\mathbb{I}_{(\cdot)} \in \{0, 1\}$  denote the indicator function for the presence of the corresponding modality. The final input token sequence to LLM is formulated as:

$$\mathbf{S} = \mathbf{T}_{\text{prompt}} \left( \bigoplus_{m \in \mathcal{M}} \mathbf{H}_{\text{stim}}^{(m)} \right) \oplus (\mathbb{I}_{\text{em}} \cdot \mathbf{H}_{\text{em}}) \left( \bigoplus_{k \in \mathcal{K}} \mathbf{H}_{\text{beta}}^{(k)} \right) \oplus (\mathbb{I}_{\text{vox}} \cdot \mathbf{H}_{\text{vox}}). \quad (5)$$

where  $\oplus$  denotes the sequence concatenation operator, and terms with  $\mathbb{I} = 0$  or empty sets are omitted.

To efficiently adapt the pre-trained multimodal LLM to the neuroscientific domain, low-rank adaptation (LoRA) (Hu et al., 2022) is used, where we freeze the LLM’s original parameters and inject trainable low-rank matrices into the attention layers.

### 3.2. Training Pipeline

Building a unified model that comprehends heterogeneous brain signals and stimuli requires large-scale multimodal training. NOBEL leverages Qwen2.5-Omni (Xu et al., 2025) as the backbone, whose visual and auditory encoders are directly inherited and thus inherently aligned with the LLM’s semantic space. While this ensures robust handling of external stimuli, the task-specific fMRI branch faces a unique

challenge: decoding subtle, stimulus-evoked perceptual information via beta weights is significantly more difficult than extracting global physiological meta-information due to the low SNR. Directly mapping these noisy, high-dimensional features to the LLM space often leads to optimization instability and poor semantic grounding. To address this, we implement a targeted pre-alignment strategy for the fMRI beta branch prior to the joint multimodal training. Drawing inspiration from MindEye2 (Scotti et al., 2024), we prioritize aligning the noisy neural representations with the robust sensory features already encoded by Qwen2.5-Omni. The output features of the beta encoders and the corresponding frozen stimuli encoders are projected into a shared low-dimensional latent space. A contrastive objective is applied to maximize the similarity between the brain signal embeddings and their corresponding ground-truth stimulus embeddings. To mitigate the limited sample size in fMRI datasets and improve generalization, we additionally adopt MixCo-style neural feature mixing (Li et al., 2025) during pre-alignment, which interpolates neural representations and their corresponding stimulus embeddings as a form of cross-modal regularization. This process effectively utilizes the high-quality visual/audio representations as “semantic anchors” to stabilize the fMRI features. Only after this cross-modal correspondence is established are the pre-aligned features projected into the LLM input space via the MLP aligners.

With the stimulus-related branches pre-aligned, the framework proceeds to unified omni-modal instruction tuning. In this stage, data from all modalities, including EEG, MEG, raw fMRI voxels, fMRI beta weights, and external stimuli, are integrated into the dynamic sequence generation process. All decoding tasks are formulated as brain-to-text generation problems, allowing the model to learn synergistic representations across modalities. The entire system is optimized using the standard autoregressive next token prediction objective. Given the target text response  $\mathbf{Y} = \{y_1, y_2, \dots, y_L\}$ , the loss function is formulated as:

$$\mathcal{L} = - \sum_{t=1}^L \log P(y_t | y_{<t}, \mathbf{S}). \quad (6)$$

This training objective ensures that NOBEL learns to generate coherent, context-aware analysis conditioned on the unified omni-modal brain dynamics, while the use of LoRA allows for efficient adaptation of the LLM backbone to the neuroscientific domain.

## 4. Experimental Setup

### 4.1. Data Specifications

To construct a versatile foundation model capable of decoding the full spectrum of brain dynamics, a diverse corpus

of datasets was aggregated to serve as the training substrate. As detailed in Table 1, this collection spans high-frequency EEG and MEG signals and low-frequency fMRI maps. While standard clinical datasets such as AD65 and ABIDE-I are included to establish baseline competencies in physiological analysis, specific emphasis is placed on several specialized data categories introduced to endow the model with fine-grained and multimodal abilities.

First, to address the challenge of cross-modal synthesis, scarce paired datasets are incorporated to enable joint learning across different signal types. Specifically, the LEMON (Babayán et al., 2019) and Nat-View (Telesford et al., 2023) datasets are utilized for joint EEG-fMRI processing, while the SMN4Lang (Wang et al., 2022) dataset is employed for MEG-fMRI tasks. The SomatoMotor (Lin et al., 2025) dataset is included to facilitate joint EEG-MEG learning.

Besides, to foster precision signal understanding beyond coarse classification, specialized tasks are designed using the HCP (Van Essen et al., 2013) dataset by injecting random perturbations ranging from 1% to 10% of the fMRI signal amplitude. The model is required to identify the specific perturbed brain regions and regress the corresponding perturbation magnitudes, a process that necessitates the capture of fine-grained variations within the neural dynamics.

To enable the model to capture and interpret the dynamic variations in brain signals induced by external stimuli, the NSD (Allen et al., 2022) and HAD (Zhou et al., 2023) datasets are included. Utilizing the beta-encoding stream, these datasets are employed to map specific stimulus-evoked neural patterns to their corresponding high-level semantic content. The training formulation includes generative decoding, where the model translates stimulus-driven brain activity directly into image captions or video classifications, and stimulus-brain verification, which requires distinguishing whether a specific visual input triggered the recorded neural response. Dataset details are included in Appendix B.

### 4.2. Model and Training Specifications

The NOBEL framework is instantiated based on Qwen2.5-Omni-7B (Xu et al., 2025). To inherit strong multimodal capabilities, the LLM backbone, as well as the audio and visual stimuli encoders, are initialized with pre-trained weights from Qwen2.5-Omni-7B. For the brain signal branches, we leverage domain-specific foundation models. The unified EMEG encoder is initialized from BrainOmni-base (Xiao et al., 2025), and the fMRI task-agnostic voxel encoder is initialized from NeuroSTORM (Wang et al., 2025a). All remaining components are randomly initialized. Regarding the task-specific beta encoding sets  $\mathcal{M}$  and  $\mathcal{K}$  in Eqn. (5), our implementation covers two primary categories: static images and dynamic video-audio clips. For the image-evoked beta encoder, we adopt the architecture of MindEye2 (Scotti

## One Brain, Omni Modalities: Towards Unified Non-Invasive Brain Decoding with Large Language Models

Table 1. Overview of the used datasets. The collection spans single-modality clinical datasets, pioneering paired EEG/MEG-fMRI datasets, and complex stimulus-aware semantic decoding datasets. To make a comparison with previous literature, balance accuracy (BAcc) is used to evaluate EEG/MEG classification tasks, while accuracy (Acc) is primarily used to evaluate other classification tasks. We use mean absolute error (MAE) to evaluate HCP stimulus amplitude regression and Rouge-L score to evaluate NSD image captioning.

Modality	Dataset	Task	Duration	#Subject	#Train Sample	#Test Sample	Metric $\uparrow$
<i>High-Frequency Electromagnetic Datasets</i>							
EEG	AD65	Alzheimer’s Disease Detection	14.9h	65	3.1k	1.1k	BAcc%
	MDD	Depression Detection	20.3h	35	4.5k	1.4k	BAcc%
	PD31	Parkinson’s Disease Detection	2.5h	31	0.6k	0.1k	BAcc%
	TUAB	Abnormal Signal Detection	1135.7h	2328	299.1k	36.9k	BAcc%
	TUEV	Event Type Classification	155.9h	294	68.7k	28.3k	BAcc%
	FACED	Emotion Recognition	28.7h	123	6.3k	2.0k	BAcc%
	WBCIC_SHU	Motor Imagery Classification	34.0h	51	18.6k	6.0k	BAcc%
MEG	PhysioNet-MI	Motor Imagery Classification	10.9h	109	6.1k	1.9k	BAcc%
	ASD74	Autism Spectrum Disorder	34.2h	74	7.8k	2.2k	BAcc%
EEG + MEG	MEG-MMI	Depression Detection	14.8h	51	1.1k	0.3k	BAcc%
EEG + MEG	SomatoMotor	Motor Response Prediction	0.7h	5	0.7k	0.2k	BAcc%
<i>Low-Frequency Metabolic Datasets</i>							
fMRI (Voxel-based)	ABIDE-I	Autism Detection (asd)	111.8h	1035	19.7k	2.4k	Acc%
		Gender Classification (sex)					Acc%
	ADHD200	ADHD Detection (adhd)	129.5h	973	19.4k	3.1k	Acc%
		Depression Detection (mdd)					Acc%
	Neural Processing	Gender Classification (sex)	21.2h	39	2.9k	0.8k	Acc%
		Schizophrenia Detection (scz)					Acc%
	Working Memory	Gender Classification (sex)	35.2h	99	4.7k	1.5k	Acc%
		Gender Classification (sex)					Acc%
	XP1-2	Gender Classification (sex)	13.0h	30	2.8k	1.2k	Acc%
		Brain Area Classification (area)					Acc%
HCP	Stimulus Amplitude Reg. (amp)	418.3h	1096	108.2k	9.5k	MAE	
<i>Synergistic Omni-Modal Datasets</i>							
EEG + fMRI (Voxel-based)	LEMON	Gender Classification	39.6h	220	6.0k	0.5k	Acc%
MEG + fMRI (Voxel-based)	Nat-View	Gender Classification	42.8h	22	8.1k	1.7k	Acc%
MEG + fMRI (Voxel-based)	SMN4Lang	Gender Classification	70.4h	12	13.6k	9.6k	Acc%
<i>Stimulus-Aware Datasets</i>							
fMRI (Beta-based)	NSD	Image Captioning	284h	8	29.9k	21.1k	Rouge-L
Stimuli + fMRI (Beta-based)	HAD	Video Classification	31.2h	30	19.4k	2.2k	Acc%
Stimuli + fMRI (Beta-based)	NSD	Image-Brain Verification	284h	8	59.8k	42.1k	Acc%
Stimuli + fMRI (Beta-based)	HAD	Video-Brain Verification	31.2h	30	38.8k	4.3k	Acc%

et al., 2024), while for the video-evoked one, we utilize a lightweight MLP as the encoder.

For pre-alignment for the fMRI beta branch, we use dataset-specific training protocols for NSD and HAD. For the NSD dataset, we use a minibatch size of 128, evenly distributed across 8 subjects. The model is trained with an initial learning rate of  $1 \times 10^{-4}$  and a cosine cyclic scheduler. Training is conducted for 150 epochs. MixCo-based neural feature mixing is applied during the first 50 epochs of pre-alignment only. For the HAD dataset, we use a minibatch size of 32 and an initial learning rate of  $1 \times 10^{-3}$  using a OneCycle scheduler. Pre-alignment on HAD is formulated as a 180-way classification and trained using a cross-entropy loss.

For joint multimodal training, to adapt this massive archi-

ture to the neuroscientific domain efficiently, we employ LoRA with the rank and alpha set to  $r = 128, \alpha = 256$ . Optimization is applied to the LoRA, the fMRI encoders, and all modality aligners. Other parameters are kept frozen to preserve their generalizable representations. The model is first trained with a learning rate of  $2 \times 10^{-5}$  and a global batch size of 32 for a total of 90,000 steps with a linear scheduler, then fine-tuned on specialized data. To mitigate the optimization instability caused by the extreme heterogeneity of the input signals, we implement a modality-aware batch sampling strategy, ensuring that all samples within a single training batch belong to the same modality. For inference, we employ a greedy decoding strategy to generate deterministic text responses. The datasets and specific evaluation metrics used are provided in Table 1.

## 5. Experimental Results

### 5.1. Results on EEG, MEG, or voxel-based fMRI Tasks

Table 2 and Table 3 present the quantitative evaluation of NOBEL on unimodal EEG, MEG, and fMRI tasks. When interpreting these results, it is crucial to acknowledge that conventional baselines are typically specialized models, trained and optimized exclusively on single datasets for isolated tasks, while NOBEL is architected as a unified, omni-modal foundation model designed to integrate heterogeneous signals within a shared semantic space.

Despite this architectural difference, NOBEL demonstrates strong competitiveness. For EEG and MEG tasks, as shown in Table 2, it consistently outperforms established discriminative baselines such as ST-Transformer and SPaRCNet across the majority of EEG and MEG benchmarks. Furthermore, even when compared against the current state-of-the-art BrainOmni, NOBEL still exhibits competitive performance. Notably, on AD65 and TUAB, NOBEL achieves accuracies of 81.3% and 82.4%, respectively, surpassing BrainOmni. This suggests the potential of our generative framework for aligning high-frequency electromagnetic features with the rich semantic space of an LLM.

In the voxel-based fMRI domain, as detailed in Table 3, NOBEL exhibits a similar pattern of resilience and capability. Specifically, on gender classification tasks across the ABIDE-I, Neural Processing, and XP1-2 datasets, NOBEL achieves accuracies of 89.2%, 83.6%, and 78.8%, respectively, consistently surpassing both the NeuroSTORM and SWiFT baselines. This indicates that the unified framework effectively captures global phenotypic traits, potentially benefiting from the regularization provided by the LLM’s semantic space to generalize better across subjects. Regarding pathology detection tasks such as autism, ADHD, depression, and schizophrenia, NOBEL also delivers competitive performance, maintaining robustness comparable to specialized encoders. Notably, on the HCP benchmark focusing on perturbed brain area classification and stimulus amplitude regression, NOBEL matches the high precision of the NeuroSTORM encoder, which demonstrates that our model successfully retains the capabilities of the underlying encoder. This confirms that the alignment process preserves the precision required to perceive subtle, low-level information in fMRI, without losing granularity during the projection to the semantic space.

### 5.2. Results on stimuli-aware beta-based fMRI tasks

Table 4 summarizes the performance on stimulus-aware tasks using the HAD and NSD datasets. These tasks are categorized into two settings: fMRI only decoding, and stimuli-input cross-modal verification.

In the fMRI only decoding setting, the model interprets se-

mantic content solely from brain signals. For the HAD video classification task, NOBEL achieves an accuracy of 74.6%, which is competitive with the specialized MLP baseline. On the more challenging NSD image captioning task, NOBEL demonstrates robust semantic understanding with a Rouge-L score of 29.7 across all subjects. It is important to note that the MindEye2 baseline is only for a single-subject split. In contrast, NOBEL handles a multi-subject setting simultaneously. Although evaluating on heterogeneous functional topography across multiple subjects is more challenging than modeling a single subject, our model still achieves high linguistic correspondence. Appendix A visualizes qualitative examples of these decoded captions.

For the stimuli-input cross-modal verification setting, which involves processing both external stimuli and brain signals, NOBEL demonstrates unique capabilities. Since stimuli and fMRI reside in distinct modalities, existing baselines struggle to process them concurrently. However, by aligning omni-modal signals within the semantic space of the LLM, NOBEL effectively analyzes the relationship between the sensory input and the neural response. In this task, the model determines whether a specific image or video triggered the recorded fMRI signal. NOBEL achieves an accuracy of 62.8% on HAD and reaches 92.7% on NSD. The high accuracy on NSD indicates that the model has successfully learned a precise alignment between visual features and their corresponding cortical representations, enabling it to verify the causal link between stimulus and brain activity.

### 5.3. Synergistic Omni-Modal Decoding

The most significant distinction between NOBEL and existing brain foundation models lies in its capability to synthesize heterogeneous signals. While previous works are confined to isolated modalities, NOBEL bridges the “frequency gap”, integrating electromagnetic signals with metabolic maps. To validate this synergistic capability, we evaluate the model on paired datasets where cross-modal recordings are available. Table 5 presents the comparative results.

Across all benchmarks, NOBEL consistently outperforms the best-performing single-modality baselines. On LEMON and SMN4Lang, the joint model leverages the complementary nature of the signals to boost accuracy beyond what is achievable by either EEG-MEG or fMRI alone. This trend is even more pronounced on the Nat-View dataset, where the EEG-only branch yields below-chance performance (16.7%), likely because the data relies heavily on spatial features that scalp-EEG fails to capture. Rather than being hampered by the weaker modality, the joint model utilizes the fMRI information while extracting subtle temporal cues from the EEG, pushing the final accuracy to 92.8%. These results validate that NOBEL does not merely average the outputs of separate encoders. Instead, the LLM backbone acts as a semantic integrator, effectively aligning the

Table 2. Quantitative results on EEG and MEG tasks of our model and specialized discriminative baselines, including CNN-Transformer (Peh et al., 2022), ContraWR (Yang et al., 2023), SPaRCNet (Jing et al., 2023), ST-Transformer (Song et al., 2021), LaBraM (Jiang et al., 2024), CBraMod (Wang et al., 2025b), FAMED (Hirano et al., 2024), and BrainOmni (Xiao et al., 2025).

Model	EEG								MEG		EEG + MEG
	AD65	MDD	PD31	TUAB	TUEV	FACED	WBCIC.SHU	PhysioNet-MI	ASD74	MEG-MMI	SomatoMotor
CNN-Transformer	77.7	86.9	50.0	80.7	32.3	36.8	65.8	32.9	50.0	50.0	50.0
ContraWR	78.8	81.9	45.8	81.2	41.3	33.6	59.3	36.4	50.3	52.8	50.0
SPaRCNet	60.3	79.9	40.4	78.5	40.8	37.2	73.4	45.8	51.1	57.3	53.7
ST-Transformer	61.2	79.6	50.0	79.5	40.7	39.4	75.5	39.9	60.5	<b>57.4</b>	66.2
LaBraM	62.9	86.1	50.0	81.2	60.5	45.7	80.4	53.7	-	-	-
CBraMod	72.3	84.9	73.7	81.3	57.2	42.0	79.7	57.8	-	-	-
FAMED	-	-	-	-	-	-	-	-	51.3	50.0	50.0
BrainOmni	80.3	<b>89.1</b>	<b>82.5</b>	81.7	<b>64.5</b>	<b>49.7</b>	<b>82.1</b>	<b>58.4</b>	<b>65.3</b>	55.8	<b>92.1</b>
NOBEL	<b>81.3</b>	85.9	74.5	<b>82.4</b>	61.7	41.2	79.4	49.1	63.6	54.2	81.3

Table 3. Quantitative results on voxel-based fMRI tasks of our model and other fMRI encoder baselines, including BrainGNN (Li et al., 2021), BrainHarmonix-F (Dong et al., 2025), SWiFT (Kim et al., 2023), and NeuroSTORM (Wang et al., 2025a). Baselines marked with (\*) are from Dong et al. (2025), which may have different data splits from our settings and are included only for reference. NOBEL demonstrates competitive performance in phenotype prediction and retains precise low-level signal perception on HCP.

Model	ABIDE-I		ADHD200	Neural Processing		Working Memory		XP1-2	HCP	
	asd	sex	adhd	mdd	sex	scz	sex	sex	area	amp
BrainGNN*	56.7	-	62.2	-	-	-	-	-	-	-
BrainHarmonix-F*	57.4	-	<b>67.7</b>	-	-	-	-	-	-	-
SWiFT	49.1	86.7	60.8	50.0	75.0	75.3	76.4	70.3	36.8	0.48
NeuroSTORM	57.1	85.4	56.1	<b>73.7</b>	75.0	<b>80.6</b>	<b>80.5</b>	66.9	100	0.04
NOBEL	<b>57.6</b>	<b>89.2</b>	56.9	61.7	<b>83.6</b>	72.1	79.1	<b>78.8</b>	<b>100</b>	<b>0.01</b>

Table 4. Results on stimulus-aware semantic tasks. We compare (i) fMRI-only decoding (classification for HAD and captioning for NSD) and (ii) stimuli-conditioned classification (verifying whether the given stimuli triggered fMRI). Note that the MindEye2\* baseline is reported on a single-subject split, whereas NOBEL is evaluated in a more challenging multi-subject setting.

Model	fMRI only		fMRI + stimuli	
	HAD	NSD	HAD	NSD
MLP baseline	78.0	-	-	-
MindEye2*	-	32.6	-	-
NOBEL	74.6	29.7	62.8	92.7

millisecond-level dynamics of EEG-MEG with the voxel-level topology of fMRI within a shared semantic space.

## 6. Conclusion

This paper introduces NOBEL, the first foundation LLM designed to unify non-invasive high-frequency EEG-MEG signals and low-frequency fMRI signals within a generative LLM framework. By orchestrating a unified EEG-MEG encoder and a novel dual-path fMRI strategy, NOBEL supports the comprehensive processing of EEG, MEG, and fMRI, while simultaneously integrating external audio-visual stimuli into a shared semantic space. Our extensive experimental evaluation confirms that NOBEL operates as a robust generalist: it not only retains the discriminative capacity of single-

Table 5. Results on synergistic cross-modal tasks. We compare the model trained on isolated modalities versus joint inputs. Results show that synthesizing EEG-MEG and fMRI signals consistently yields superior performance compared to using either alone.

Model	EEG + fMRI		MEG + fMRI
	LEMON	Nat-View	SMN4Lang
EEG-MEG-only baseline	70.6	16.7	77.4
fMRI-only baseline	76.1	86.6	69.0
NOBEL (EEG-MEG + fMRI)	<b>81.8</b>	<b>92.8</b>	<b>78.5</b>

modal encoders across standard physiological tasks but also unlocks cross-modal capabilities unattainable by isolated models. Compelling empirical evidence is provided that the synergistic fusion of EEG-MEG and fMRI yields superior decoding accuracy through cross-modal complementarity, outperforming unimodal baselines. The model also excels in stimulus-aware tasks, achieving robust performance in decoding visual semantics from multi-subject fMRI data on NSD and HAD. Uniquely, the incorporation of external stimuli as inputs endows the model with semantic reasoning powers, enabling it to verify the causal link between sensory inputs and neural responses. By processing EEG-MEG and fMRI brain dynamics in a single model, NOBEL takes a step towards unifying non-invasive brain decoding, showing the potential of omni-modal brain understanding.

## Impact Statement

This paper presents work whose goal is to advance the field of Machine Learning. There are many potential societal consequences of our work, none which we feel must be specifically highlighted here.

## References

- Allen, E. J., St-Yves, G., Wu, Y., Breedlove, J. L., Prince, J. S., Dowdle, L. T., Nau, M., Caron, B., Pestilli, F., Charest, I., et al. A Massive 7T fMRI Dataset to Bridge Cognitive Neuroscience and Artificial Intelligence. *Nature neuroscience*, 2022.
- Babayán, A., Erbey, M., Kumral, D., Reinelt, J. D., Reiter, A. M., Röbbing, J., Schaare, H. L., Uhlig, M., Anwänder, A., Bazin, P.-L., et al. A Mind-brain-body Dataset of MRI, EEG, Cognition, Emotion, and Peripheral Physiology in Young and Old Adults. *Scientific data*, 2019.
- Bellec, P., Chu, C., Chouinard-Decorte, F., Benhajali, Y., Margulies, D. S., and Craddock, R. C. The Neuro Bureau ADHD-200 Preprocessed Repository. *Neuroimage*, 2017.
- Chen, J., Wang, X., Huang, C., Hu, X., Shen, X., and Zhang, D. A Large Finer-grained Affective Computing EEG Dataset. *Scientific Data*, 2023.
- Chen, J., Qi, Y., Wang, Y., and Pan, G. MindGPT: Interpreting What You See With Non-invasive Brain Recordings. *IEEE Transactions on Image Processing*, 2025.
- Craddock, C., Benhajali, Y., Chu, C., Chouinard, F., Evans, A., Jakab, A., Khundrakpam, B. S., Lewis, J. D., Li, Q., Milham, M., et al. The Neuro Bureau Preprocessing Initiative: Open Sharing of Preprocessed Neuroimaging Data and Derivatives. *Frontiers in Neuroinformatics*, 2013.
- Dong, Z., Li, R., Chong, J. S. X., Dehestani, N., Teng, Y., Lin, Y., Li, Z., Zhang, Y., Xie, Y., Ooi, L. Q. R., et al. Brain Harmony: A Multimodal Foundation Model Unifying Morphology and Function into 1D Tokens. *arXiv preprint arXiv:2509.24693*, 2025.
- Esteban, O., Markiewicz, C. J., Blair, R. W., Moodie, C. A., Isik, A. I., Erramuzpe, A., Kent, J. D., Goncalves, M., DuPre, E., Snyder, M., et al. fMRIPrep: A Robust Pre-processing Pipeline for Functional MRI. *Nature methods*, 2019.
- Fadeev, K. A., Reyes, I. V. R., Goiaeva, D. D., Obukhova, T. S., Ovsiannikova, T. M., Prokofyev, A. O., Rytikova, A. M., Novikov, A. Y., Kozunov, V. V., Stroganova, T. A., and Orekhova, E. V. Perception of vowel sounds in children with autism spectrum disorders and typically developing children (MEG/ERF study. doi:10.18112/openneuro.ds005234.v2.1.7, 2024.
- Fu, Y., Gao, J., Yang, B., and Feng, J. Making Your Dreams A Reality: Decoding the Dreams into a Coherent Video Story from fMRI Signals. *arXiv preprint arXiv:2501.09350*, 2025.
- Hendrycks, D. and Gimpel, K. Gaussian Error Linear Units (GELUs). *arXiv preprint arXiv:1606.08415*, 2016.
- Hirano, R., Asai, M., Nakasato, N., Kanno, A., Uda, T., Tsuyuguchi, N., Yoshimura, M., Shigihara, Y., Okada, T., and Hirata, M. Deep Learning Based Automatic Detection and Dipole Estimation of Epileptic Discharges in MEG: a Multi-Center Study. *Scientific Reports*, 2024.
- Horikawa, T. Mind Captioning: Evolving Descriptive Text of Mental Content from Human Brain Activity. *Science Advances*, 2025.
- Hu, E. J., Shen, Y., Wallis, P., Allen-Zhu, Z., Li, Y., Wang, S., Wang, L., Chen, W., et al. LoRA: Low-rank Adaptation of Large Language Models. In *Proc. ICLR*, 2022.
- Jiang, W.-B., Zhao, L.-M., and Lu, B.-L. Large Brain Model for Learning Generic Representations with Tremendous EEG Data in BCI. In *Proc. ICLR*, 2024.
- Jing, J., Ge, W., Hong, S., Fernandes, M. B., Lin, Z., Yang, C., An, S., Struck, A. F., Herlopian, A., Karakis, I., et al. Development of Expert-level Classification of Seizures and Rhythmic and Periodic Patterns During EEG Interpretation. *Neurology*, 2023.
- Kan, X., Cui, H., Lukemire, J., Guo, Y., and Yang, C. FB-NETGEN: Task-aware GNN-based fMRI Analysis via Functional Brain Network Generation. In *Proc. MIDL*, 2022a.
- Kan, X., Dai, W., Cui, H., Zhang, Z., Guo, Y., and Yang, C. Brain Network Transformer. In *Proc. NeurIPS*, 2022b.
- Kawahara, J., Brown, C. J., Miller, S. P., Booth, B. G., Chau, V., Grunau, R. E., Zwicker, J. G., and Hamarneh, G. BrainNetCNN: Convolutional Neural Networks for Brain Networks; Towards Predicting Neurodevelopment. *NeuroImage*, 2017.
- Kim, P., Kwon, J., Joo, S., Bae, S., Lee, D., Jung, Y., Yoo, S., Cha, J., and Moon, T. Swift: Swin 4D fMRI Transformer. *Proc. NeurIPS*, 2023.
- Lepping, R. J., Atchley, R. A., Chryssikou, E., Martin, L. E., Clair, A. A., Ingram, R. E., Simmons, W. K., and Savage, C. R. Neural Processing of Emotional Musical and Nonmusical Stimuli in Depression. *PLoS one*, 2016.

- Li, S., Jin, Z., Zhang, R.-Y., Gu, S., and Li, Y. Predictive Vision-language Integration in The Human Visual Cortex. *bioRxiv*, 2025.
- Li, X., Zhou, Y., Dvornek, N., Zhang, M., Gao, S., Zhuang, J., Scheinost, D., Staib, L. H., Ventola, P., and Duncan, J. S. BrainGNN: Interpretable Brain Graph Neural Network for fMRI Analysis. *Medical Image Analysis*, 2021.
- Lin, F.-H., von Pechmann, D. F., Lankinen, K., Ahlfors, S., Rosen, B., Ahveninen, J., Hämäläinen, M., and Raij, T. Somatomotor. doi:10.18112/openneuro.ds006035.v1.0.0, 2025.
- Lioi, G., Cury, C., Perronnet, L., Mano, M., Bannier, E., Lécuyer, A., and Barillot, C. Simultaneous EEG-fMRI During a Neurofeedback Task, a Brain Imaging Dataset for Multimodal Data Integration. *Scientific data*, 2020.
- Liuzzi, L., Chang, K., Keren, H., Zheng, C., Saha, D., Nielson, D., and Stringaris, A. Mood Induction in MDD and Healthy Adolescents. doi:10.18112/openneuro.ds003568.v1.0.4, 2023.
- Miltiadous, A., Tzimourta, K. D., Afrantou, T., Ioannidis, P., Grigoriadis, N., Tsalikakis, D. G., Angelidis, P., Tsipouras, M. G., Glavas, E., Giannakeas, N., and Tzallas, A. T. A dataset of 88 EEG recordings from: Alzheimer’s disease, Frontotemporal dementia and Healthy subjects. doi:10.18112/openneuro.ds004504.v1.0.2, 2023.
- Mumtaz, W. MDD Patients and Healthy Controls EEG Data (New). doi: 10.6084/m9.figshare.4244171.v2, 2016. URL <https://doi.org/10.6084/m9.figshare.4244171.v2>.
- Obeid, I. and Picone, J. The Temple University Hospital EEG Data Corpus. *Frontiers in Neuroscience*, 2016.
- Ouahidi, Y. E., Lys, J., Thölke, P., Farrugia, N., Padeloup, B., Gripon, V., Jerbi, K., and Lioi, G. REVE: A Foundation Model for EEG—Adapting to Any Setup with Large-Scale Pretraining on 25,000 Subjects. *arXiv preprint arXiv:2510.21585*, 2025.
- Ozcelik, F. and VanRullen, R. Natural Scene Reconstruction from fMRI Signals Using Generative Latent Diffusion. *Scientific Reports*, 2023.
- Peh, W. Y., Yao, Y., and Dauwels, J. Transformer Convolutional Neural Networks for Automated Artifact Detection in Scalp EEG. In *Proc. EMBC*, 2022.
- Radford, A., Kim, J. W., Hallacy, C., Ramesh, A., Goh, G., Agarwal, S., Sastry, G., Askell, A., Mishkin, P., Clark, J., et al. Learning Transferable Visual Models from Natural Language Supervision. In *Proc. ICML*, 2021.
- Repovš, G. and Barch, D. M. Working Memory Related Brain Network Connectivity in Individuals with Schizophrenia and Their Siblings. *Frontiers in human neuroscience*, 2012.
- Rockhill, A. P., Jackson, N., George, J., Aron, A., and Swann, N. C. UC San Diego Resting State EEG Data from Patients with Parkinson’s Disease. doi:10.18112/openneuro.ds002778.v1.0.5, 2021.
- Schalk, G., McFarland, D. J., Hinterberger, T., Birbaumer, N., and Wolpaw, J. R. BCI2000: A General-purpose Brain-computer Interface (BCI) system. *IEEE Transactions on Biomedical Engineering*, 2004.
- Scotti, P., Banerjee, A., Goode, J., Shabalin, S., Nguyen, A., Dempster, A., Verlinde, N., Yundler, E., Weisberg, D., Norman, K., et al. Reconstructing The Mind’s Eye: fMRI-to-image with Contrastive Learning and Diffusion Priors. *Proc. NeurIPS*, 2023.
- Scotti, P. S., Tripathy, M., Torrico, C., Kneeland, R., Chen, T., Narang, A., Santhirasegaran, C., Xu, J., Naselaris, T., Norman, K. A., and Abraham, T. M. MindEye2: Shared-Subject Models Enable fMRI-To-Image With 1 Hour of Data. In *Proc. ICML*, 2024.
- Song, Y., Jia, X., Yang, L., and Xie, L. Transformer-based Spatial-Temporal Feature Learning for EEG Decoding. *arXiv preprint arXiv:2106.11170*, 2021.
- Takagi, Y. and Nishimoto, S. High-resolution Image Reconstruction with Latent Diffusion Models from Human Brain Activity. In *Proc. CVPR*, 2023.
- Tang, J., LeBel, A., Jain, S., and Huth, A. G. Semantic Reconstruction of Continuous Language from Non-invasive Brain Recordings. *Nature Neuroscience*, 2023.
- Telesford, Q. K., Gonzalez-Moreira, E., Xu, T., Tian, Y., Colcombe, S. J., Cloud, J., Russ, B. E., Falchier, A., Nentwich, M., Madsen, J., et al. An Open-access Dataset of Naturalistic Viewing Using Simultaneous EEG-fMRI. *Scientific Data*, 2023.
- Van Essen, D. C., Smith, S. M., Barch, D. M., Behrens, T. E., Yacoub, E., Ugurbil, K., Consortium, W.-M. H., et al. The WU-Minn Human Connectome Project: An Overview. *Neuroimage*, 2013.
- Wang, C., Jiang, Y., Peng, Z., Li, C., Bang, C., Zhao, L., Lv, J., Sepulcre, J., Yang, C., He, L., et al. Towards a General-purpose Foundation Model for fMRI Analysis. *arXiv preprint arXiv:2506.11167*, 2025a.
- Wang, J., Zhao, S., Luo, Z., et al. CBraMod: A Criss-Cross Brain Foundation Model for EEG Decoding. In *Proc. ICLR*, 2025b.

- Wang, S., Zhang, X., Zhang, J., and Zong, C. A Synchronized Multimodal Neuroimaging Dataset for Studying Brain Language Processing. *Scientific Data*, 2022.
- Wei, Y., Zhang, Y., Xiao, X., Qian, C., Wang, T., and Calhoun, V. D. fMRI-LM: Towards a Universal Foundation Model for Language-Aligned fMRI Understanding. *arXiv preprint arXiv:2511.21760*, 2025.
- Xiao, Q., Cui, Z., Zhang, C., Chen, S., Wu, W., Thwaites, A., Woolgar, A., Zhou, B., and Zhang, C. BrainOmni: A Brain Foundation Model for Unified EEG and MEG Signals. In *Proc. NeurIPS*, 2025.
- Xu, J., Guo, Z., He, J., Hu, H., He, T., Bai, S., Chen, K., Wang, J., Fan, Y., Dang, K., et al. Qwen2.5-Omni Technical Report. *arXiv preprint arXiv:2503.20215*, 2025.
- Yang, B., Rong, F., Xie, Y., Li, D., Zhang, J., Li, F., Shi, G., and Gao, X. A Multi-day and High-quality EEG Dataset for Motor Imagery Brain-computer Interface. *Scientific Data*, 2025.
- Yang, C., Xiao, C., Westover, M. B., and Sun, J. Self-supervised Electroencephalogram Representation Learning for Automatic Sleep Staging: Model Development and Evaluation Study. *JMIR AI*, 2023.
- Yang, F., Feng, C., Wang, D., Wang, T., Zeng, Z., Xu, Z., Park, H., Ji, P., Zhao, H., Li, Y., et al. NeuroBind: Towards Unified Multimodal Representations for Neural Signals. *arXiv preprint arXiv:2407.14020*, 2024.
- Yi, K., Wang, Y., Ren, K., and Li, D. Learning Topology-Agnostic EEG Representations with Geometry-Aware Modeling. In *Proc. NeurIPS*, 2023.
- Zhou, M., Gong, Z., Dai, Y., Wen, Y., Liu, Y., and Zhen, Z. A Large-scale fMRI Dataset for Human Action Recognition. *Scientific Data*, 2023.

## A. Caption Case

Fig .2 provides some examples of text captions generated by NOBEL from fMRI signals on the NSD dataset.

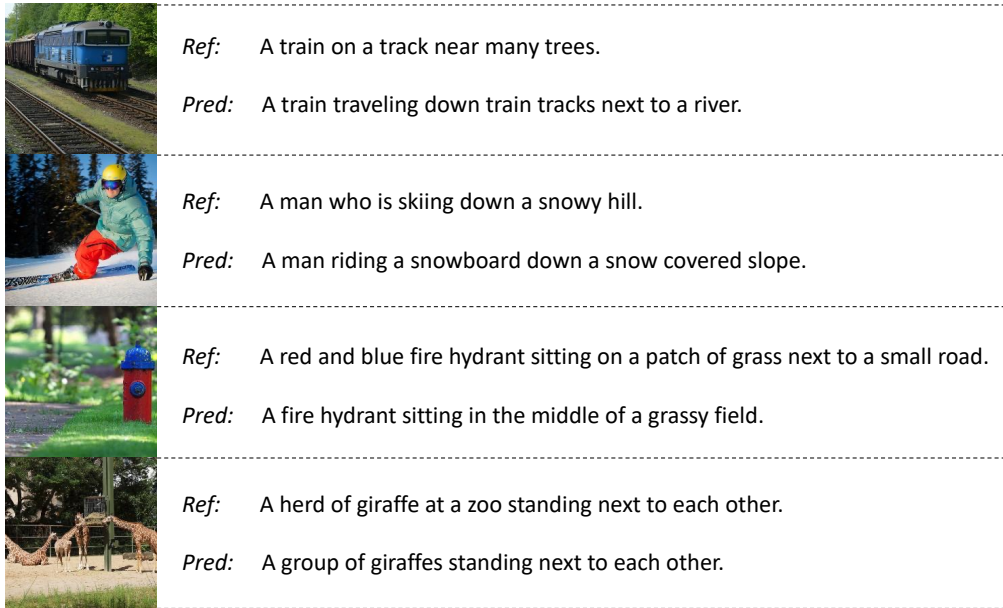


Figure 2. Examples of NOBEL decoding results on NSD. Each case displays the original visual stimulus presented to the subject alongside the reference caption and the model’s predicted caption. These demonstrate that NOBEL can predict semantically accurate image descriptions directly from brain activity.

## B. Details of Datasets

In this section, we provide detailed descriptions of the datasets utilized for the instruction tuning and evaluation of NOBEL:

**AD65** (Miltiadous et al., 2023): AD65 consists of resting-state EEG recordings collected from 36 patients with Alzheimer’s disease and 29 healthy controls. Signals were recorded using 19 channels at 500 Hz. The dataset provides 5349 segments of 10 seconds, which are used for binary classification of Alzheimer’s disease.

**MDD** (Mumtaz, 2016): This dataset includes EEG recordings from 35 patients diagnosed with major depressive disorder and 30 healthy controls, collected using 20 channels at 256 Hz. Data were recorded under three conditions: eyes open, eyes closed, and task engagement. In total, 7302 samples of 10-second duration are used to train a classifier for distinguishing MDD patients from controls.

**PD31** (Rockhill et al., 2021): The PD31 dataset contains resting-state EEG data collected from 16 healthy controls and 15 individuals with Parkinson’s disease, using 32 channels at 512 Hz. A total of 882 segments of 10 seconds are extracted to support binary classification for Parkinson’s disease diagnosis.

**TUAB** (Obeid & Picone, 2016): TUAB is a large-scale EEG dataset consisting of recordings from 2328 subjects, acquired with 21 channels at a sampling rate of 256 Hz. Each recording is annotated as either normal or abnormal. For the downstream task, 408,853 non-overlapping 10-second segments are extracted and used to perform binary classification of EEG normality.

**TUEV** (Obeid & Picone, 2016): The TUEV dataset contains EEG signals collected from 294 individuals using 21 channels at 256 Hz. The recordings are divided into 112,237 segments of 5 seconds, each labeled as one of six event categories: spike and sharp wave (SPSW), generalized periodic epileptiform discharges (GPED), periodic lateralized epileptiform discharges (PLED), eye movement (EYEM), artifact (ARTF), or background activity (BCKG). A multi-class classification task is conducted to identify these event types.

**FACED** (Chen et al., 2023): FACED consists of EEG recordings from 123 subjects watching 28 emotion-inducing video clips, covering nine emotion categories. Signals are recorded using 30 channels at either 1000 Hz or 250 Hz. For evaluation,

the original labels are mapped to three coarse-grained classes (negative, neutral, and positive), yielding 10,332 samples of 10 seconds for emotion classification.

**WBCIC\_SHU** (Yang et al., 2025): The WBCIC\_SHU dataset comprises high-density EEG recordings (58 channels, 1000 Hz) from 51 participants performing motor imagery tasks involving left- and right-hand grasping. A total of 30,591 segments, each lasting 4 seconds, are extracted for a binary classification task to recognize the imagined movement type.

**PhysioNet-MI** (Schalk et al., 2004): PhysioNet-MI provides EEG data recorded from 109 subjects using 64 channels at a sampling rate of 160 Hz during motor imagery and motor execution experiments. The dataset includes four distinct task conditions. A total of 9837 4-second segments are employed to classify the corresponding motor tasks.

**ASD74** (Fadeev et al., 2024): ASD74 is a MEG dataset comprising recordings from 35 children diagnosed with autism spectrum disorder and 39 typically developing children. Data were acquired with 306 channels at 1000 Hz while participants watched videos accompanied by auditory stimuli. In total, 12,320 10-second segments are used to classify ASD versus typical development.

**MEG-MMI** (Liuzzi et al., 2023): The MEG-MMI dataset includes MEG recordings acquired from 29 adolescents with major depression and 22 healthy controls during mood induction experiments. Data were recorded using 269 magnetometer channels at 1200 Hz. A total of 1770 segments, each 30 seconds long, are used to classify the presence of major depression.

**SomatoMotor** (Lin et al., 2025): The SomatoMotor dataset includes simultaneous EEG (74 channels) and MEG (306 channels) recordings from five subjects, sampled at 1004 Hz. During the experiment, participants received electrical stimulation to the right median nerve and were instructed to lift the left index finger as quickly as possible. A total of 1208 2-second samples are used to distinguish stimulus-induced finger movements from spontaneous ones.

**ABIDE-I** (Craddock et al., 2013): The ABIDE-I dataset includes preprocessed resting state fMRI recordings from 505 individuals suffering from autism spectrum disorders (ASD) and 530 typical controls. A total of 25181 16-second samples were used for gender classification and classification to predict the presence of ASD.

**ADHD200** (Bellec et al., 2017): The ADHD200 dataset includes preprocessed resting state fMRI recordings from 362 children and adolescents diagnosed with ADHD and 585 typically developing controls. A total of 23321 20-second samples were used for classification to predict the presence of ADHD.

**Neural Processing** (Lepping et al., 2016): The Neural Processing Dataset includes functional MRI (fMRI) recordings from 19 individuals with major depressive disorder (MDD) and 20 never-depressed (ND) control participants, who listened to standardized musical and nonmusical stimuli during scanning. A total of 3832 20-second samples were used for gender classification and classification to predict the presence of MDD.

**Working Memory** (Repovš & Barch, 2012): The Working Memory dataset includes task-based fMRI data during three working memory loads (0-back, 1-back, 2-back) of an N-back task from 23 individuals suffering from schizophrenia (SCZ) and 76 typical controls. A total of 6336 20-second samples were used for gender classification and classification to predict the presence of SCZ.

**XP1-2** (Lioi et al., 2020): The XP1 and XP2 dataset include fMRI from right-handed, neurofeedback (NF)-naive healthy individuals during motor imagery NF tasks. A total of 2237 20-second fMRI samples were used for gender classification.

**HCP** (Van Essen et al., 2013): The HCP dataset includes imaging data from approximately 1,200 healthy young adults. All functional data used in this work are preprocessed and aligned to the MNI space. The resting-state fMRI data were acquired with a repetition time (TR) of 0.8 s. During scanning, participants were instructed to remain at rest. Each subject completed one or two resting-state sessions. To construct supervised learning targets, we adopt the Yeo’s 7-network cortical parcellation. For each sample, we introduce a controlled bias to regions within a selected functional network and treat the corresponding network index together with the bias magnitude as labels.

**LEMON** (Babayan et al., 2019): The LEMON dataset includes EEG(62-channels, 2.5kHz) and preprocessed resting state fMRI recordings from 227 subjects. A total of 11173 20-second EEG samples and 7139 20-second fMRI samples were used for gender classification.

**Nat-View** (Telesford et al., 2023): The Nat-View dataset includes simultaneous EEG(61 channels, 5kHz) and preprocessed fMRI recordings from 22 subjects. Recordings cover tasks including 12Hz flickering checkerboard, resting state, Inscapes animation, naturalistic videos, and PEER calibration. A total of 7705 20-second EEG and fMRI samples were used for

gender classification.

**SMN4Lang** (Wang et al., 2022): The SMN4Lang dataset includes MEG(306-channels, 1000Hz) and fMRI recordings from the same 12 subjects while the subjects listened to 6 hours of naturalistic stories. A total of 12684 20-second EEG and fMRI samples were used for gender classification.

**NSD** (Allen et al., 2022): The NSD dataset contains 7T fMRI recordings from eight subjects viewing natural images. The functional data have an isotropic spatial resolution of 1.8 mm and a repetition time of 1.6 s. Each subject contributed on average approximately 35.5 hours of scanning, corresponding to 26,625 stimulus trials. Event-level neural responses are estimated using a general linear model, from which beta weights are derived. In this study, we follow the dataset split in Mindeye2.

**HAD** (Zhou et al., 2023): The HAD dataset consists of 3T fMRI recordings from 30 subjects. Functional images were acquired with an isotropic spatial resolution of 2 mm and a repetition time (TR) of 2 s. During the experiment, participants viewed short action videos spanning 180 action categories, with four distinct 2-second clips presented for each category. All subjects' functional data were spatially normalized to the MNI space. Event-related neural responses were estimated using a general linear model. The resulting representations were used for cross-subject action category classification.

All raw fMRI data were preprocessed using fMRIPrep (Esteban et al., 2019). For all datasets, the initial steps included normalizing the data to the Montreal Neurological Institute (MNI) space and standardizing each 3D volume to a 96×96×96 size with a 2×2×2 mm spatial resolution. For fMRI sequences with mismatched original spatial resolution or TR, we first resampled the data to the target resolution, then cropped or padded the volumes to unify all of them to 96×96×96.

For MEG data, we used minimal standardized preprocessing to maximize data usability. First, a 0.1–96 Hz bandpass filter and 50/60 Hz notch filters were applied to remove slow signal drifts and power line noise; for MEG recordings with HPI coils, extra filtering was added for their corresponding HPI frequency bands. All signals were then resampled to a 250 Hz sampling rate. Bad channels were identified with a power spectral density-based detection algorithm and then interpolated for repair. To address inconsistent reference values and large amplitude fluctuations, we subtracted the reference value from all sensors of the same type for each sampling point, and normalized each channel to a zero mean and unit variance at the sampling level. Sensor coordinates and orientations were obtained from either the positions provided with the dataset or the device's standard montage.